On Using Residual Voltage to Estimate Electrode Model Parameters for Damage Detection

Ashwati Krishnan[1], *Student Member, IEEE* , Shawn K. Kelly[2], *Senior Member, IEEE*

***Abstract*—Current technology has enabled a significant increase in the number of electrodes for electrical stimulation. For large arrays of electrodes, it becomes increasingly difficult to monitor and detect failures at the stimulation site. In this paper, we propose the idea that the residual voltage from a biphasic electrical stimulation pulse can serve to recognize damage at the electrode-tissue interface. We use a simple switch circuit approach to estimate the relaxation time constant of the electrode model, which essentially models the residual voltage in biphasic electrical stimulation, and compare it with standard electrode characterization techniques. Out of 15 electrodes in a polyimide-based SIROF array, our approach highlights 3 damaged electrodes, consistent with measurements made using cyclic voltammetry and electrode impedance spectroscopy.**

I. INTRODUCTION

Chronically implantable electrical stimulation mechanisms have been the focus of physiological engineering research for the last decade. Many devices have been clinically deployed for years, such as cochlear implants. With the advent of microelectronics, it has become imperative to look into the criticality of safe functional electrical stimulation for large electrode arrays. A stimulating electrode is exposed to a wide variety of dangers such as structural failure and scar tissue growth. Damage can occur if there is exposure to electrode potential much higher than the water window. Stimulation electrode characteristics can also change due to electrode dissolution on prolonged use [1]. Moreover, with large stimulation arrays such as those in retinal prosthetics, monitoring the status of different electrodes becomes challenging. Currently, the only established mechanism for safety in an electrode is to short the electrode immediately after stimulation. The elegance of the shorting method lies in its simplicity, because the electronic switch is the most inexpensive hardware that could be added to a circuit. However, the method is very brute-force, and it essentially nulls a voltage measurement that may give us a clue about the health of the interface. Shorting the electrode out may prevent us from detecting early damage in implanted electrodes.

The basic model for the electrode/electrolyte interface depicts the most significant contributors to the mechanism of charge transfer in stimulation electrodes (Fig. 1). We briefly describe the basis for this model and highlight the double layer capacitance and the charge transfer resistance as the first order containers of electrode interface information. We then describe the biphasic stimulus current waveform, a waveform which is commonly used for electrical stimulation. We present measurement data on interface characteristics in saline, in order to empirically validate the idea of using residual voltage to detect damage in stimulation electrodes.

*Research supported in part by the Department of Veterans Affairs (VA), the Pennsylvania Infrastructure Technology Alliance (PITA), Sigma Xi Grants-in-Aid of Research (GIAR), and the Institute for Complex Engineered Systems, Carnegie Mellon University. MOSIS provides in-kind foundry services.

[1]Ashwati Krishnan is with the Department of Electrical and Computer Engineering and the Institute of Complex Engineered Systems (ICES), Carnegie Mellon University, Pittsburgh, PA 15213, USA. Email: ashwatik@andrew.cmu.edu

[2]Shawn K. Kelly is with the VA Pittsburgh, PA 15240, USA, and with the Institute of Complex Engineered Systems, Carnegie Mellon University, Pittsburgh, PA 15213, USA. Email:skkelly@cmu.edu

II. BACKGROUND

When an electrode is placed near tissue, current flow is determined by the flow of electrons in the electrode and flow of ions in the tissue. The electrode/electrolyte (tissue) interface is modeled as shown in Fig. 1. The solution resistance, R_s, models the resistance of the bulk electrolyte. The capacitor, C_{dl}, models the double layer of charge that exists at the electrode/electroyte (tissue) interface. The charge transfer resistance, R_{ct}, in parallel with the capacitance, C_{dl}, accounts for the conduction of charged particles through the interface. The conduction of these charged particles can occur through various mechanisms, typically through oxidation-reduction reactions at the electrode for efficient stimulation electrodes [2]. While more complex models of the interface exist, we have adopted a linear charge-transfer element model to enable a practical understanding of the interface. A chronological evolution of circuit models used to depict the electrode-electrolyte/tissue interface is covered in [3].

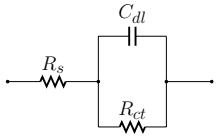

Fig. 1: Electrode-tissue interface model.

Functional electrical stimulation is performed using biphasic current pulses (Fig. 2) because it allows for better charge control. The residual voltage after the end of the anodic pulse for a *balanced* biphasic current pulse for a capacitor with a zero initial condition [4] is given by equation (1),

$$v_c(t_{a+}) = IR_{ct}[1 + e^{-(T_c+T_a+T_i)/\tau} - e^{-(T_a+T_i)/\tau} - e^{-(T_a)/\tau}], \quad (1)$$

where $\tau = R_{ct} \times C_{dl}$. Observe from (1) that the voltage at the end of the anodic pulse of a biphasic stimulation pulse contains the parameters R_{ct} and C_{dl}, which captures information about the electrode-tissue interface, and not just

978-1-4799-7234-0/15/$31.00 ©2015 IEEE

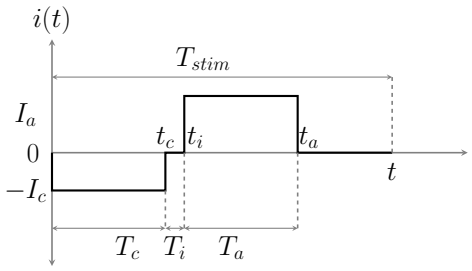

Fig. 2: General biphasic current pulse; A charge balanced biphasic current pulse is characterized by $Q_c = Q_a$, where $Q = I \times T$.

the biphasic mismatch error between anodic and cathodic pulses. In this paper, we propose that the residual voltage is a preliminary indicator of electrode damage using simple measurements.

III. PROPOSED METHOD

The main contribution of this work is to highlight the usefulness of measuring the residual voltage after a biphasic stimulus, as a way of detecting any changes to the electrode/electrolyte (tissue) interface in a chronic stimulation implant. There are several advantages to this approach: Firstly, the residual voltage is one of the most accessible measurements that is a function of R_{ct} and C_{dl}. Secondly, the dynamic range for detection of residual voltage is smaller than measuring the entire stimulation waveform. Residual voltage values after a biphasic stimulation pulse, range in the order of a few millivolts, as opposed to solution resistance (R_s) measurements, which can be in the order of volts. This makes it easier to develop low-power hardware circuits for the measurements. Thirdly, the measurement is performed *after* the stimulation pulse. Because the stimulation frequency of most applications is of the order of $100Hz$, state of the art microelectronics can acquire fairly accurate samples at frequencies that are greater by at least 2 orders of magnitude. In contrast, the standard practice of shorting mechanism uses a switch to bypass any residual charge in the form of current away from the electrode after the stimulation is complete. When the shorting switch is active, the voltage on the electrode will be clamped at zero, we thereby lose information about the electrode/electrolyte (tissue) interface.

The residual voltage represents the discharge of the double layer capacitance, C_{dl}, across the charge transfer resistance, R_{ct}. In order to determine the parametric values of the electrode/electrolyte (tissue) model (shown in Fig. 1), we analyze the transient response of the first order model to observe the *relaxation* time constant of the double-layer capacitance and the charge transfer resistance. In this section, we derive the electrical equations that are used to calculate the parametric values.

Consider the circuit shown in Fig. 3. We observe the responses of the circuit when the switch, $S1$, is closed, and when it is open. We require two equations for the solution of the model parameters, to solve for R_{ct} and C_{dl}, which

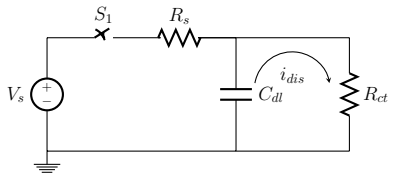

Fig. 3: Step-down switch circuit for electrode model parameter estimation

we obtain by performing two experiments. Firstly, when the switch S_1 is closed, the circuit reaches steady state, where there is no current through C_{dl}. We measure the DC current at steady state. Therefore, we arrive at the equation in (2),

$$I_s = \frac{V_s}{(R_s + R_{ct})} \tag{2}$$

Once the capacitor, C_{dl}, has charged upto $V_c = V_s \times \frac{R_{ct}}{(R_s+R_{ct})}$, switch S_1 is opened and the capacitor discharges via the charge transfer resistance. The capacitor discharge is modeled as a first order differential equation written by equating the current in the loop, which solves to the form in (4), using $v_c(0) = V_c$ as the initial condition of the capacitor.

$$C_{dl}\frac{dv_c}{dt} = -\frac{v_c}{R_{ct}} \tag{3}$$

$$v_c(t) = V_c e^{-\frac{t}{\tau}} \tag{4}$$

We estimate the relaxation time constant graphically by calculating the intercept of the tangent at the instant of discharge, as shown in Fig. 4.

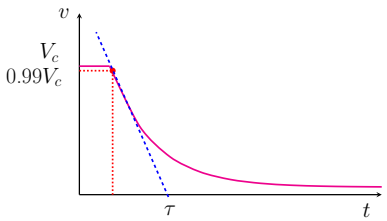

Fig. 4: Estimation of decay time constant

Thirdly, we obtain the value of the solution resistance from the step increase in the voltage response of the biphasic current stimulus waveform [4], [5]. We use this systematic methodology to estimate the parameters for the first order model shown in Fig. 1.

IV. EXPERIMENTAL SETUP

We present a three step parameter estimation method, summarized in Fig. 5. The main theoretical equations used are presented in Section III.

A. Electrodes & Experimental Setup

The electrodes used in this experiment are circular **S**puttered **Ir**idium **O**xide **F**ilm (SIROF) electrodes, which have a diameter of $400\mu m$ and were developed for retinal prosthesis

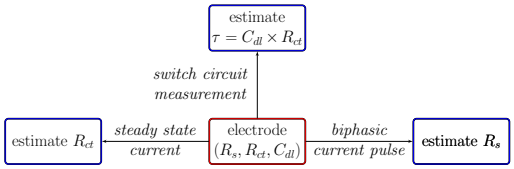

Fig. 5: Three fold method of estimating the Randle's model parameters.

devices by the Boston Retinal Implant Project [6]. The water window potential limits of SIROF electrodes are +0.8V/-0.6V [5]. The geometric surface area of each SIROF electrode is $0.125mm^2$. We used a polyimide-base electrode array (Fig. 6), with numbers identifying each of the 15 electrodes. We used a platinum counter electrode (Basi Inc. MW1033), which has a total geometric surface area of $360mm^2$, when completely immersed in the electrolyte. For the analysis and experiments in this paper, we have assumed that the potential difference across the counter electrode is negligible when compared to the working electrode.

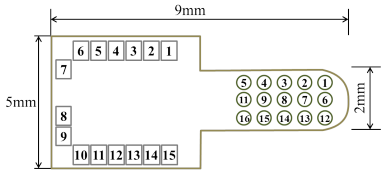

Fig. 6: SIROF electrode array with 15 electrodes (numbered)

Our electrochemical setup comprised of the SIROF working electrode, and a coiled platinum (Pt) counter electrode, in 1X physiological buffered saline (PBS) saline solution. We used the Metrohm Autolab analyzer to perform steady state current measurement, single biphasic current measurements, using a two electrode setup. Additionally, we used a three electrode setup for Cyclic Voltammetry (CV) and Electrode Impedance Spectroscopy (EIS) experiments with the Autolab measurement system, with an Ag/AgCl reference electrode (Basi Inc. MF2052) to characterize the electrode array. Cyclic voltammery was done within the water window (-0.6V/0.8V) at a scan rate of $0.1V/s$.

1) Switch Circuit Measurement (τ): The relaxation time constant measurement system is shown in Fig. 7. We obtained transient discharge curves for 15 electrodes for step voltages of $\pm 0.3V$ and $\pm 0.4V$, using the Agilent DSO7012B with a minimum sampling rate of $20kS/s$, We smoothed the data using a moving average filter and numerically obtained the time constant for tangents drawn at 99% of the step voltage.

2) Steady State Current ($R_s + R_{ct}$): We measured the steady state current of 15 electrodes, each for 20 seconds for DC voltages of $\pm 0.3V$ and $\pm 0.4V$. We averaged the steady state current and calculated the resistance ($R_s + R_{ct}$) at these voltage levels.

3) Biphasic Current Measurement (R_s): We used the Metrohm Autolab setup to generate biphasic current stimulation pulses to determine the solution resistance, R_s, from the response of the electrode/electrolyte (tissue) interface to a step change in current. We used a biphasic current pulse with

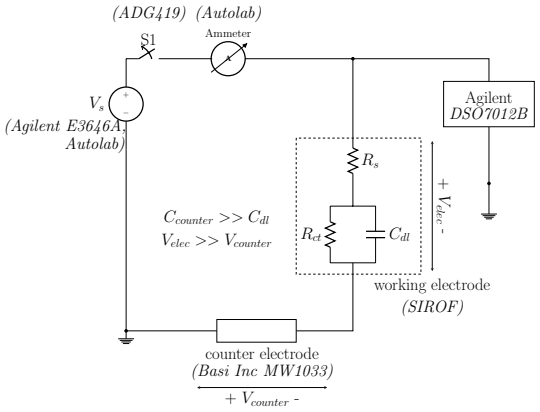

Fig. 7: Two electrode measurement setup for step response measurements.

time intervals of $5ms$ ($T_c = T_i = T_a = 5ms$), and $\pm 100\mu A$ currents ($I_a = I_c = \pm 100\mu A$).

V. RESULTS

We show the evaluation of 15 SIROF electrodes in 1X PBS using the methods described in Section IV. In order to corroborate the relationship between the residual voltage and the electrode/electrolyte (tissue) interface characteristics, we present results from Cyclic Voltammetry (CV) and Electrode Impedance Spectroscopy (EIS) characterizations in Fig. 9.

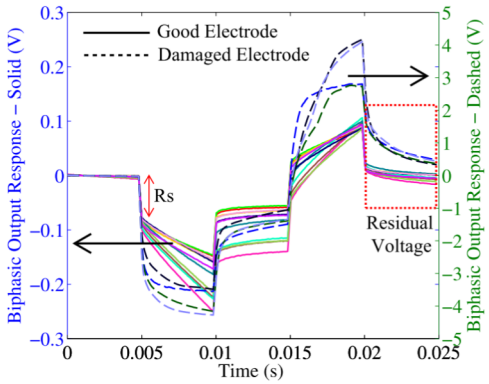

Fig. 8: Biphasic pulses for 15 electrodes, shown on different axes, due to the variation in magnitude.

The relaxation time constant obtained from the tangential method at $\pm 0.3V$ and $\pm 0.4V$ and the mean charge transfer resistance values calculated from steady state current measurements are shown in Figs. 10(a) and (b). The solution resistance values obtained from biphasic current response curves of the electrodes is shown in Fig. 10(c). The biphasic response of all electrodes is shown in Fig. 8.

VI. DISCUSSION

For all the electrodes in the presented SIROF electrode array, the CV characterization and EIS data in Fig. 9 show that electrodes 4, 7 and 8 have very high impedance and low charge capacity. The triangular markers in Fig. 10 indicate that

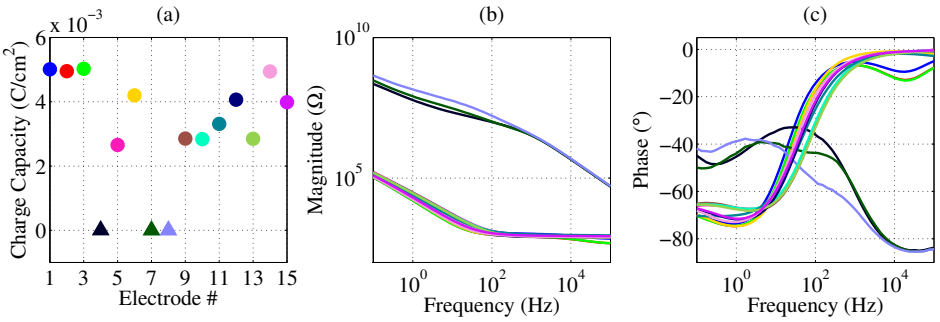

Fig. 9: (a) Charge capacity from CV measurements (b),(c) Magnitude and Phase plots from EIS measurements

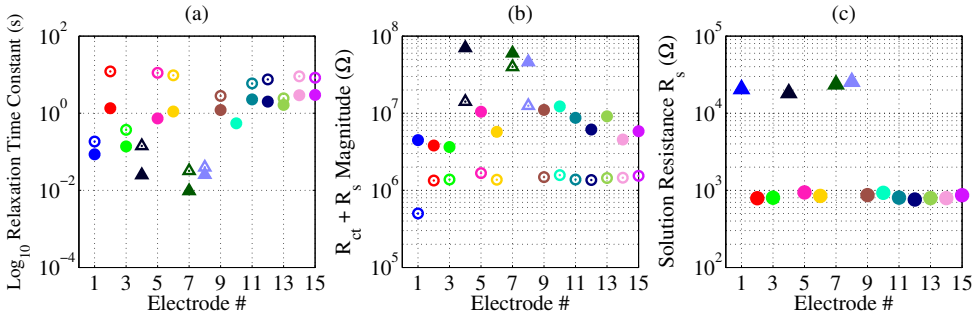

Fig. 10: (a) Measured τ values (b) Calculated $R_{ct} + R_s$ values (Filled markers indicate values measured with a positive bias (0.3,0.4), hollow markers are from measurements at negative bias (-0.3,-0.4)) (c) R_s obtained graphically from the biphasic response. Electrode #1 was exposed to excess potential after CV and EIS, but before the R_s measurement.

the relaxation time constant (τ), R_{ct} and R_s values obtained from the switch experiments render the same electrodes ineffective for stimulation. We include measurements of τ made at different electrode biases to show that there is a dependence of the electrode parameters on DC voltage level, a discussion of which is beyond the scope of this paper. The biphasic pulses shown in Fig. 8 evidently shows that the residual voltage between electrodes 4, 7 and 8 is higher when compared to the other electrodes. We would like to inform the reader that electrode #1 suffered an accidental exposure to a high potential after its characterization and before the R_s measurement, which is why the biphasic pulse in Fig. 8 (and hence the solution resistance in Fig. 10(c)) is inconsistent with the data for electrode #1 shown in Fig. 9 and Fig. 10 (a),(b). However, we decided to include the data point to highlight that any damage that can occur during electrode use, and that the residual voltage can serve as the earliest indicator of damage.

VII. CONCLUSION & FUTURE WORK

Applications such as a 1000+ electrode retinal implant are not very far into the future. The problem of electrode monitoring becomes increasingly challenging with scaling of technology. It therefore becomes necessary to know the status of each electrode easily, and as early as possible, before potential damage can occur. We empirically show that residual voltage contains first-order information about the status of the electrode/electrolyte (tissue) interface. Measuring residual voltage presents fewer design and power constraints on integrated circuit measurement circuits, allowing for low-power circuit design as well as increased compatibility with scaling of microelectrode array. We are currently working on long-term damage tests *in vitro* saline and *in vivo* tissue order to study the validity of residual voltage measurements to detect the formation of localized scar tissue.

REFERENCES

[1] S. Negi, R. Bhandari, R. V. Wagenen, and F. Solzbacher, "Factors affecting degradation of sputtered iridium oxide used for neuroprosthetic applications," *IEEE 23rd International Conference on Micro Electro Mechanical Systems*, 2010.

[2] D. R. Merrill, M. Bikson, and J. G. Jefferys, "Electrical stimulation of excitable tissue: design of efficacious and safe protocols," *Journal of Neuroscience Methods*, vol. 141, pp. 171–198, 2005.

[3] L. A. Geddes, "Historical evolution of circuit models for the electrode-electrolyte interface," *Annals of Biomedical Engineering*, vol. 25.

[4] A. Krishnan and S. Kelly, "On the cause and control of residual voltage generated by electrical stimulation of neural tissue," *34th Annual International Conference of the IEEE Engineering in Medicine and Biology Society*, pp. 3899 – 3902, 2012.

[5] S. F. Cogan, "Neural stimulation and recording electrodes," *Annual Review of Biomedical Engineering*, vol. 10, pp. 275–309, 2008.

[6] D. B. Shire *et al.*, "Development and implantation of a minimally invasive wireless subretinal neurostimulator," *IEEE Transactions on Biomedical Engineering*, vol. 56, pp. 2502–2511, 2009.